

Assessment of Grey-Field Photoelasticity

Jon Lesniak
Mike Zickel
Dan Bazile
Brad Boyce

Stress Photonics
3002 Progress Rd.,
Madison WI 53716

1.0 Introduction

The usefulness of the Grey-Field Polariscopes (GFP) has been demonstrated for subfringe photoelasticity, where low loads are used and direct measurement of strain is straightforward[1]. In most applications, there is no difficulty in controlling the load so that the strains in regions of interest are completely subfringe. However, in some applications the load can not be easily stepped and multi-fringe data must be analyzed. This paper introduces an RGB approach to analyzing multi-fringe data. Although residual stress inspection in automotive glass is a topic of its own, data from several window inspections is used here to illustrate the RGB multi-fringe approach. This data will be used to understand the nonlinear outputs of over-range data taken in high strain, hence multi-fringe, applications.

2.0 Review of technology

The grey field polariscopes illuminate the test article with circularly polarized light [2]. In the presence of birefringence the light returns elliptically polarized with the major axis oriented $\pi/4$ off the direction of the first principal strain (Fig.1).

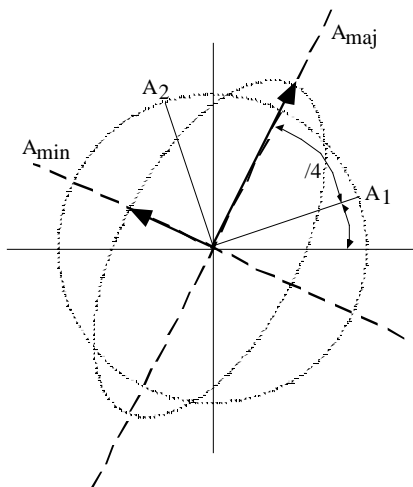


Fig. 1. Response to birefringence

An analyzer positioned in front of a video camera is rotated at an angular frequency ω . It is assumed that the analyzer is parallel with the reference orientation at $t=0$. In terms of time, the intensity map is described by

$$I = \frac{a^2}{2} [1 + \sin 2(\omega t - \epsilon) \sin \delta] \quad (1)$$

From this relation it can be seen that in the absence of birefringence ($\delta = 0$) the output is a neutral grey. It can also be seen that in the presence of birefringence the amplitude of the signal oscillates about this neutral grey level. The oscillating portion of the signal is zero when the axis of the analyzer coincides with the principal strain axes. The orientation of the first principal strain direction to the reference direction (ϵ) is related to δ by

$$\epsilon = 2\delta \quad (2)$$

A video lock-in algorithm determines the amplitude and phase of the oscillating light signal. The oscillating perturbation from grey, as seen in Fig. 1, is normalized by the grey level or the illumination intensity, which is measured as the average over the oscillation period. Therefore, the GFP output is independent of light intensity and is more closely related to the retardation angles. In general, the silver coating is not perfectly efficient in retaining polarization and extreme light intensities of dark or bright are not met. This effect is similar over the test area and is accounted for in the normal calibration procedure.

3.0 RGB Approach

As the retardation values or the spectral bandwidth increase, it is more accurate to derive the total signal as the integral of all oscillating signals over the spectral bandwidth (Fig. 2). This relation shows a decay in the peak amplitude of multi-fringe values. Because illumination effects have been removed, the relative values of the peaks can be used to identify the fringe order.

In the case of inspection of clear objects of known thickness, RGB photoelasticity[3] can be extended to the GFP. Figure 2 shows the relation between outputs of the three colors vs.

retardation. Notice blue shows the attenuating fringe values most dramatically as the bandwidth is the same for the red and green but the center wavelength of blue is significantly shorter.

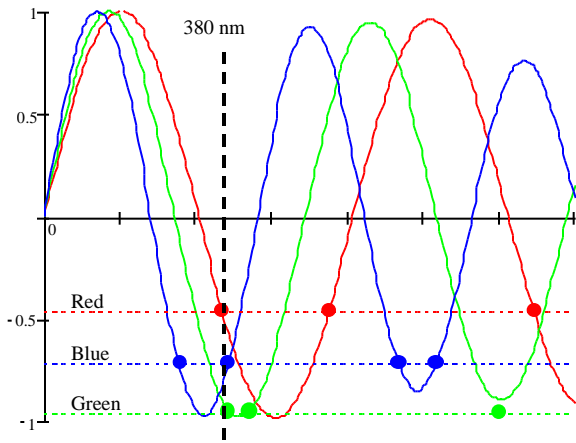
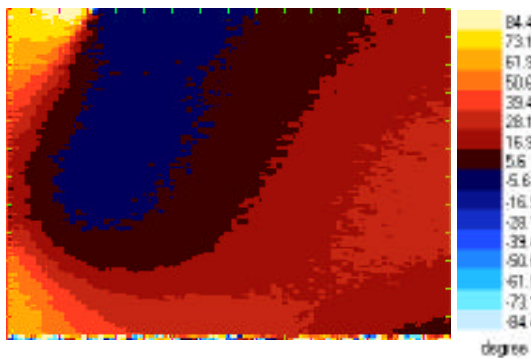
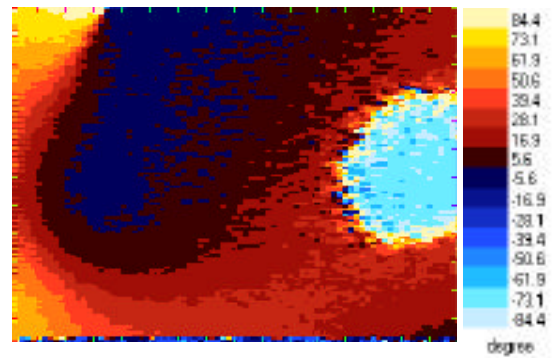


Fig. 2. Location 1 relative response

An explanation of the sign in Fig. 2 is necessary. Under subfringe operation the output of the GFP yields amplitude and phase information. The plots of Fig. 2 demonstrate the relation of both these quantities. As the magnitude of the birefringence crosses the half wave border the phase of the oscillation changes by 180 degrees or the oscillation changes sign. The direction of the principal stress, related by Eq. 2, flips 90 degrees, essentially pointing in the direction of the second principal stress instead of the first. All wavelengths yield the same direction until the birefringence of the blue light exceeds the half wave mark. Once blue crosses the half wave mark it yields a direction changed by 90°, so that the direction of blue is now opposite that of red and green. At each retardation there is a unique combination of direction and amplitude. Figure 3 is an example of the direction data in which we can see that the blue plot has flipped its direction by 90 degrees in the high stress region. This indicates that it has crossed zero and is now negative.



a) Direction of red stress



b) Direction of blue stress

Fig. 3. Direction plots

4.0 Data analysis

In a demonstration of the GFP's capabilities, Stress Photonics has inspected two locations on an automotive window containing high residual stresses. This report will discuss the two locations in detail. As demonstrated in the figures below, high levels of residual strain result in multi-fringe birefringence.

4.1 Location 1

At location 1, the relative values normalized by the peak values for 1/4 wave birefringence were

Red	+/- 0.46
Green	+/- 0.90
Blue	+/- 0.72

In Fig. 2, these values are plotted on the response curves of the system. The true fringe order is the value that satisfies all three response levels

As can be seen, the retardation at location one is 380nm. With a thickness of 2 x 4.28mm (.168") and a birefringence coefficient of 2.2 psi-in/nm, the calibration constant is 6.54/nm retardation. This yields a stress value at location 1 of 17.1 MPa (2485 psi). Although this type of analysis is performed pixel by pixel without regard to neighboring pixels, verification can be gained by looking at the data in a broader sense. Figure 4 shows the maximum in-plane shear as measured by red light. These data images show magnitude, while the direction or sign of the data is obtained from the direction image. In effect, the data is the absolute value of the responses described in Fig. 2. Line plots are the actual data across the feature and are not intended to resemble Fig. 2 which shows the output as the stress increases linearly. The stress states indicated in the following examples are hot spots that peak in the center. As can be seen by the line plot in Fig. 4 the red stress magnitude rises to a peak at 1/4 wave, drops through zero at a 1/2 wave, then rises half way up, before it falls back through zero and rises to another peak.

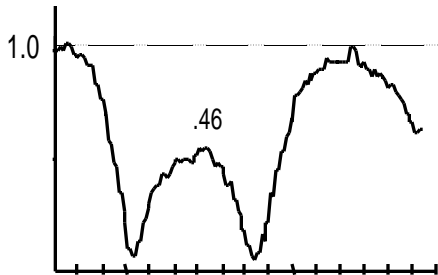
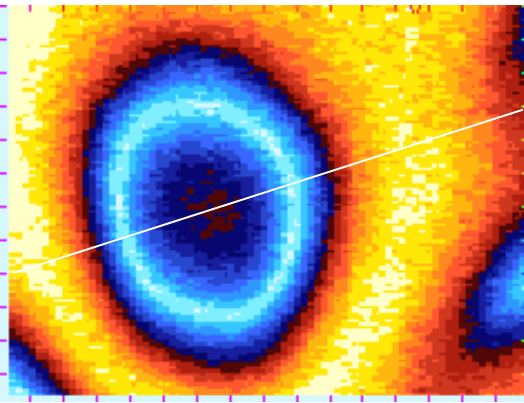


Fig. 4. Red stress response at location 1

The green data follows the same trend, but rises to nearly the peak value in the center (Fig. 5).

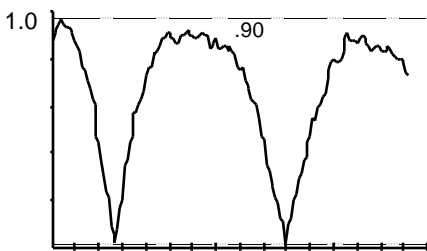
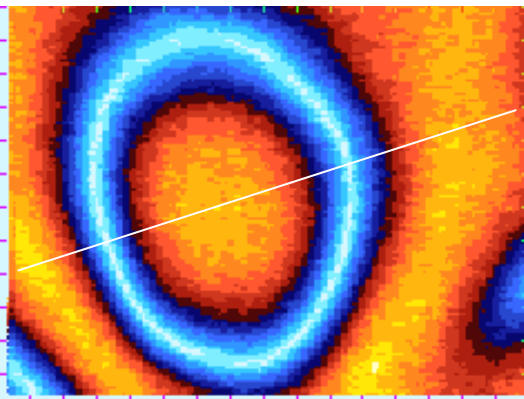


Fig. 5. Green stress response at location 1

The blue value rises up to exceed the peak in the center and actually results in a volcano appearance as the value dips back down in the center (Fig 6).

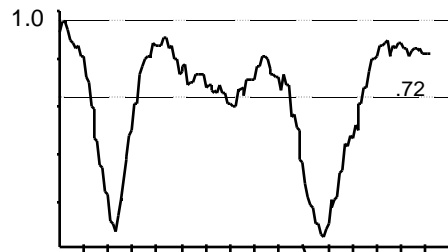
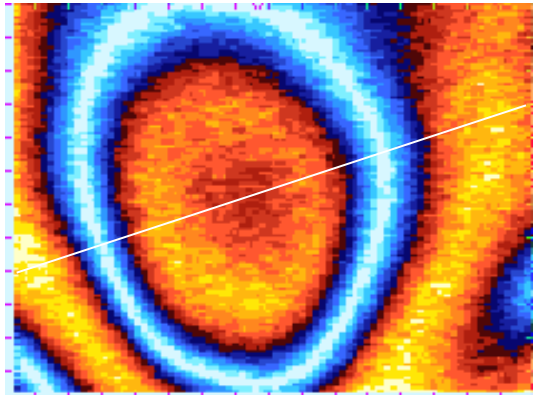


Fig 6. Blue stress response at location 1

4.2 Location 2

Similar analysis is performed in location 2. The relative values for location 2 are

Red	+/- 0.64
Green	+/- 0.23
Blue	-/+ 0.47

If these are charted relative retardation is 265nm resulting in a stress of 11.9 MPa (1733 psi) (Fig. 7)

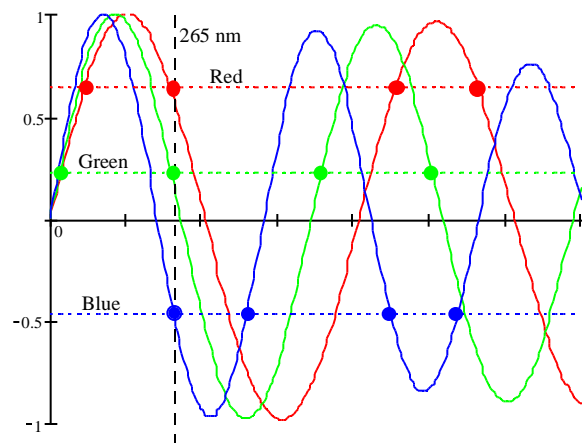
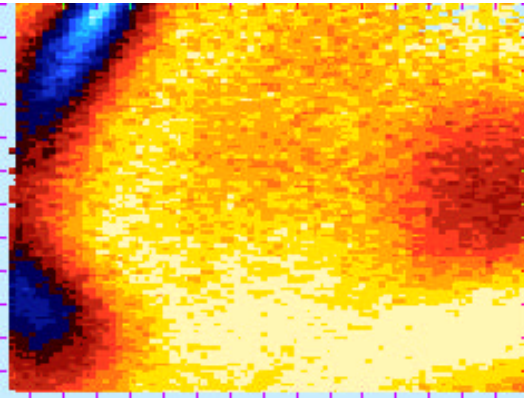
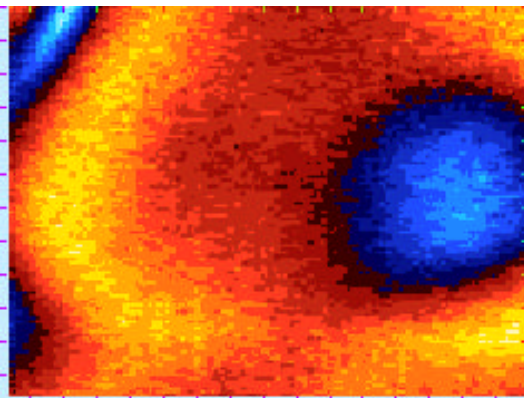


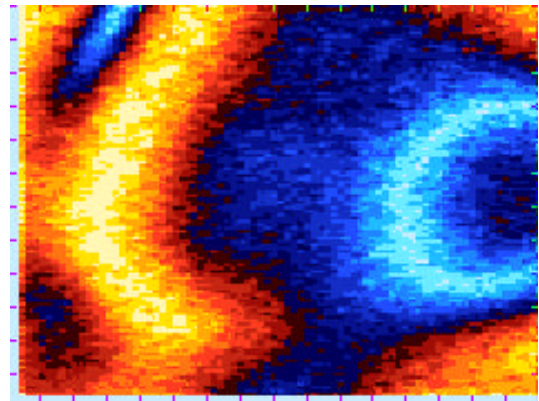
Figure 7. Relative responses at location 2



a) Red shear max



b) Green shear max



c) Blue shear max

Fig. 8. Magnitude response at location 2 R,G,B

As in location 1, fig. 8 shows the data as magnitude and the sign is determined by the direction plots as were shown in figure 3.

5.0 Conclusion

Through the use of an RGB approach the GFP's operational range can be extended to include multi-fringe applications. To further improve the system, color filters can be chosen specifically for this application. This would include a longer red color to further improve overall range. The three color system has the range to perform windshield inspections, but can be challenged by some of the more extreme values present in tempered glass.

6.0 References

- [1] Lesniak, J. R., Zickel, "Applications of automated grey-field polariscope," Proceedings of the 1998 SEM Spring Conference on Experimental Mechanics, Houston, TX, June 1-3, 1998, 298-301.
- [2] Lesniak, J. R., Zickel, M. J., Welch, C. S., Johnson, D. F., "An Innovative Polariscope for Photoelastic Stress Analysis," Proceedings of the 1997 SEM Spring Conference on Experimental Mechanics,, Bellevue, WA, June 2-4, 1997, 219-224.
- [3] Redner, S., "New Automatic Polariscope System," Experimental Mechanics, December, 486-491, 1974.